Gabriel-constrained Parametric Surface Triangulation

Oscar E. Ruiz, Carlos Cadavid, Juan G. Lalinde, Ricardo Serrano, Guillermo Peris-Fajarnés

Abstract—The Boundary Representation of a 3D manifold contains FACES (connected subsets of a parametric surface $S : \mathbb{R}^2 \longrightarrow \mathbb{R}^3$). In many science and engineering applications it is cumbersome and algebraically difficult to deal with the polynomial set and constraints (LOOPs) representing the FACE. Because of this reason, a Piecewise Linear (PL) approximation of the FACE is needed, which is usually represented in terms of triangles (i.e. 2-simplices). Solving the problem of FACE triangulation requires producing quality triangles which are: (i) independent of the arguments of S, (ii) sensitive to the local curvatures, and (iii) compliant with the boundaries of the FACE and (iv) topologically compatible with the triangles of the neighboring FACEs. In the existing literature there are no guarantees for the point (iii). This article contributes to the topic of triangulations conforming to the boundaries of the FACE by applying the concept of parameter-independent Gabriel complex, which improves the correctness of the triangulation regarding aspects (iii) and (iv). In addition, the article applies the geometric concept of tangent ball to a surface at a point to address points (i) and (ii). Additional research is needed in algorithms that (i) take advantage of the concepts presented in the heuristic algorithm proposed and (ii) can be proved correct.

Keywords—surface triangulation, conforming triangulation, surface sampling, Gabriel complex.

GLOSSARY

S:	Parametric Surface. $S : \mathbb{R}^2 \to \mathbb{R}^3$. is an (infinite) 2-manifold without border.
F, H:	Faces. Connected subsets of a parametric surface ($F, H \subset S$).
$S^{-1}(F)$:	Pre-image of F in parametric space $U - V$.
T_F:	Triangulation of face F in Euclidean space.
T_{UV}:	A triangulation in parametric space $U - V$.
$T = S(T_{UV})$:	Triangulation in $\mathbb{R}^3$ as a mapping, via S, of the triangulation T_{UV} in $U - V$ parametric space.
∂X	Boundary of the set X.
L:	Loop ($L \subseteq \partial F$) is a 1-manifold without border. It is a connected subset of the boundary of F.

Oscar E. Ruiz, Carlos Cadavid, Juan Lalinde are Professors and Ricardo Serrano is a research assistant with the CAD CAM CAE Laboratory at EAFIT University, Medellín, Colombia. Guillermo Peris is Professor with the Universidad Politécnica de Valencia, Spain. E-mails: {oruiz,rserrano,ccadavid,jlalinde}@eafit.edu.co and gperis@degi.upv.es

t:	A triangle of the triangulation T.
p, q:	Points in Euclidean space. $p, q \in \mathbb{R}^3$.
u, v, w:	Real parameters of a curve $C(w)$ or a surface $S(u, v)$.
$cl(A)$:	Closure of the set A. $cl(A) = A \cup \partial A$.
$int(A)$:	Interior of the set A. $int(A) = A - \partial A$.
$B_G(p, q, r)$:	Gabriel Ball in $\mathbb{R}^3$. Spherical point set whose center is contained in the plane pqr, passing through the points $p, q, r \in R^3$.
$B_G(p, q)$:	Gabriel Ball in $\mathbb{R}^3$. Spherical point set whose center is contained in the edge pq, passing through the points $p, q \in \mathbb{R}^3$.
e:	Edge of a triangle.

I. INTRODUCTION

Boundary Representations, B-Reps, are the computer formalization of the boundary of a body ($M = \partial BODY$). Shortly, M is a collection of SHELLs, which in turn are collections of FACEs. For convenience, we will assume that the SHELLs are 2-manifolds without border in $\mathbb{R}^3$. Each SHELL is decomposed into FACEs, which must have boundary. It is customary in geometric modeling to make a FACE F a connected proper subset of *one* parametric surface $S(u, v) \subset \mathbb{R}^3$. In this article we consider the b-reps as closed 2-manifolds with continuity C^2 inside each face and C^0 among them.

The border of F is ∂F, which is the collection of LOOPs L_i embedded in S. Each LOOP L_i is split into a sequence of EDGEs E_i. The LOOP L_i can be thought of as a 1-manifold without border, with C^∞ continuity except in a finite number of points, where it is C^0-continuous. In such locations L_i is split into EDGEs E_j, each one being a C^∞ 1-manifold with border. The problem of surface triangulation takes place in one of such FACEs F. A PL approximation T_F of face F is required which: (a) is formed by triangles, (b) departs from F in less than a distance ϵ, (c) has triangles as equilateral as possible, (d) has as few triangles as possible, and, (e) each edge e_j of the triangle set has exactly two incident triangles. Property (e) is a consequence of the fact that a B-Rep is a 2-manifold without boundary. The triangulation T is also a 2-manifold (of the C^0 class) without boundary. Condition (e) also holds for edges e_j whose extremes lie on any loop L_i. This means, this edge e_i receives a triangle from the triangulation T_F (face F) and another from the triangulation T_H (face H).

An important aspect to control in triangulating a face F is that having a triangulation T_{UV} correctly covering $S^{-1}(F)$ in parametric space $U - V$ is not a guarantee for the triangulation $T = S(T_{UV})$ in $\mathbb{R}^3$ to be correct. Several problems may

arise: (i) Fig. 1 illustrates that a completely internal triangle $[a, b, c]$ in parametric space $U - V$ may not be mapped by S to an internal triangle $[S(a), S(b), S(c)]$ in $\mathbb{R}^3$. (ii) roughly equilateral triangles t in $U - V$ space may map to extremely deformed triangles $S(t)$ in $\mathbb{R}^3$ because of sharp warping caused by S, (iii) neighboring triangles $t_i, t_j, t_k, ...$ in $U - V$ space mapped via $S()$ may form a fish scale effect in R^3 because of the same warping in S.
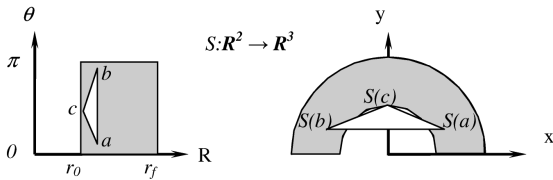
Fig. 1.   Triangle abc is internal in parameter space. Triangle $S(a)S(b)S(c)$ is external to the surface $S(r, \theta) = (r \cos(\theta), r \sin(\theta), 0)$

II. RELATED WORK

A. Fundamental definitions

As discussed in [1] a smooth 2-manifold with boundary (face) F is a sub-manifold of a smooth 2-manifold S without boundary. If the neighborhood of a point $p \in F$ is homeomorphic to a 2 dimensional euclidean space, then we say that the p is in the interior of F ($int(F)$). If the neighborhood of a point p in F is homeomorphic to a half euclidean space then we say that the point is in the boundary of F (∂F). The exterior of the submanifold F is composed by the points $p \in S$ and not in the closure of F ($p \notin cl(F)$). It includes all the points neither in the interior nor the boundary of F but still in S. The boundary is a closed set and the interior and exterior are open sets. In Fig. 4 the interior, boundary and exterior are shown ($A - B$ denotes the difference between sets A and B).
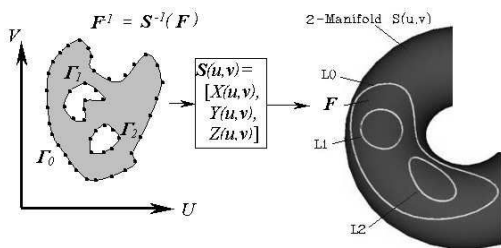

Fig. 2.   Pre-image $F^{-1} = S^{-1}(F)$ of the face F by the parametric surface S.

Fig. 2 displays the general situation in which a face F is carried by a parametric surface S in $\mathbb{R}^3$. F is a connected subset of S, with the boundary of F, $\partial F = \{L_0, ..., L_n\}$ being the set of loops L_i which limit F on S. If the function $S(u, v)$ is 1-1 (which can be guaranteed by a convenient decomposition of the overall B-Rep) then there exists a pre-image of F in parametric space $U \times V$, that we call F^{-1}. Such a region can be calculated as $F^{-1} = S^{-1}(F)$. To do so, a point sample of ∂F formed by points $p_i \in \mathbb{R}^3$

is tracked back to their pre-images $(u_i, v_i) \in (U \times V)$ therefore rendering a connected region $F^{-1} \subset (U \times V)$, most likely with holes, bounded by a set of planar Jordan curves $\partial F^{-1} = \{\Gamma_0, ..., \Gamma_n\}$.
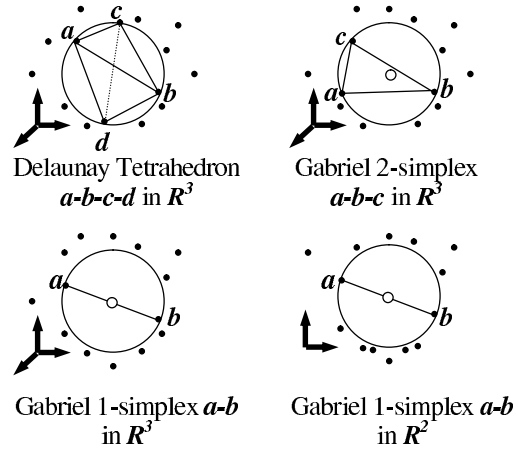

Fig. 3.   Delaunay tetrahedron for points $a, b, c, d \in \mathbb{R}^3$, 2-simplex Gabriel for $a, b, c \in \mathbb{R}^3$, 1-simplex Gabriel for $a, b \in \mathbb{R}^3$, 1-simplex Gabriel for $a, b \in \mathbb{R}^2$.

Fig. 3 displays a short collection of Delaunay and Gabriel complexes. A Delaunay tetrahedron in a set of points in 3D is a tetrahedron (3-simplex) formed by four points whose circumscribed sphere contains no other point of the set. Given vertices $v_i v_j v_k$ in the point set, they form a Gabriel triangle (2-simplex) if the smallest sphere through them contains no other point of the set. The triangle $v_i v_j v_k$ is embedded in the equatorial plane of such a sphere. A Gabriel edge $v_i v_j$ (1-simplex) is one with v_i and v_j in the point set, such that the sphere centered in $(v_i + v_j)/2$ with radius $r = d(v_i, v_j)/2$ contains no point of the sample other than v_i and v_j. Such a sphere is the smallest one containing v_i and v_j. Each 1-simplex Gabriel makes part of at least one 2-simplex Gabriel, and each 2-simplex Gabriel makes part of at least one Delaunay tetrahedra.

The present article applies the Gabriel variant (1- and 2-simplices) to Delaunay connectivity to calculate a triangulation for a point sample V_F (sensitive to curvature and independent of the parameterization) on the face F, carried by a parametric surface S. Section 2 reviews theoretical and algorithmic knowledge related to triangulations and surface curvatures. Section 3 discusses the algorithms devised and implemented to triangulate Boundary Representations. Section 4 presents five complex Boundary Representations with manufacturing and organic surfaces and high genii triangulated by the implemented algorithm. Section 5 concludes this article and sketches directions for future work.

B. Curvature Measurement in Parametric Surfaces

A parametric surface is a function $S : \mathbb{R}^2 \to \mathbb{R}^3$, which we assume to be twice derivable in every point. The derivatives

are named in the following manner ([8], [16],):

$$S_u = \frac{\partial S}{\partial u}; \ S_v = \frac{\partial S}{\partial v}; \ S_{uu} = \frac{\partial^2 S}{\partial u^2}; \ S_{vv} = \frac{\partial^2 S}{\partial v^2}; \quad (1)$$

$$S_{uv} = S_{vu} = \frac{\partial^2 S}{\partial u \partial v}; \ n = \frac{S_u \times S_v}{|S_u \times S_v|}$$

with n being the unit vector normal to the surface S at $S(u, v)$.

The Gaussian and Mean curvatures are given by:

$$K = \frac{LN - MM}{EG - FF}; H = \frac{LG - 2MF + NE}{2(EG - FF)}; \quad (2)$$

where the coefficients E, F, G, L, M, N are:

$$E = S_u \bullet S_u; \quad F = S_u \bullet S_v = S_v \bullet S_u; \quad G = S_v \bullet S_v; \quad (3)$$

$$L = S_{uu} \bullet n; \quad M = S_{uv} \bullet n; \quad N = S_{vv} \bullet n;$$

Minimal, Maximal, Gaussian, Mean Curvatures from the Weingarten Application

The Weingarten Application ([8]), W is an alternative way to calculate the Gaussian and Mean curvatures.

$$W = \begin{bmatrix} a_{11} & a_{12} \\ a_{21} & a_{22} \end{bmatrix} \quad (4)$$

with $a_{11}, a_{12}, a_{21}, a_{22}$ being:

$$a_{11} = \frac{MF - LG}{EG - F^2}; \quad a_{12} = \frac{NF - MG}{EG - F^2}; \quad (5)$$

$$a_{21} = \frac{LF - ME}{EG - F^2}; \quad a_{22} = \frac{MF - NE}{EG - F^2}$$

The following facts allow to calculate the curvature measures for S from the Weingarten Application: (i) The eigenvalues k_1 y k_2 of W are called **Principal Curvatures**, with k_1 being the *maximal* curvature and k_2 being the *minimal* curvature (assume that $|k_1| \geq |k_2|$). (ii) $K = det(W)$ is the **Gaussian Curvature**, with $K = k_1 * k_2$. (iii) $2H = trace(W)$ is twice the **Mean Curvature**, with $H = \frac{k_1 + k_2}{2}$. (iv) The maximal and minimal curvatures are: $k_1 = H + \sqrt{H^2 - K}$ and $k_2 = H - \sqrt{H^2 - K}$.

$W * v = k * v$ is the eigenpair equation for the W matrix. The solutions for such an equation are the eigenpairs (k_1, v_1) and (k_2, v_2). Therefore, $W * v_1 = k_1 * v_1$ and $W * v_2 = k_2 * v_2$. The directions of principal curvature *in $U \times V$ space* are v_1 and v_2 ($v_1 = (w_{11}, w_{12})$ and $v_2 = (w_{21}, w_{22})$). The directions of maximal and minimal curvatures in R^3 are $u_1 = w_{11} * S_u + w_{12} * S_v$ and $u_2 = w_{21} * S_u + w_{22} * S_v$, respectively.

C. Previous Work

In [10] the surface triangulation problem is addressed. The paper is the first to propose a surface triangulation with a 2D-Delaunay like method, where the circle empty of points of the sample in 2D is replaced by a sphere in 3D, defined by the 3 points and centered in the surface. The main advantage of choosing that sphere (of the many given 3 points) is that the algorithm can create more sampled points and triangles given any metric like curvature. In the paper expensive operations like surface-curve intersection are used. The triangulation is a remeshing, because of this if the triangulation created in parametric space or with another method is incorrect the

algorithm should also give an incorrect output or fail. In [12] the restricted Delaunay triangulation of general topological spaces is defined. The restricted Delaunay triangulation in the case of a 2-manifold is the dual of the Voronoi diagram intersected with the surface, a triangle is created in each intersection of 3 intersected with the surface Voronoi cells. Another contribution of the paper is to show that Chew's algorithm is a restricted Delaunay triangulation. [3] and [4] treat the reconstruction of curves in 2D and surfaces in 3D respectively. Good properties about the sampling are given, showing how the curvature and the local feature size (the smallest distance to the medial axis) have a lot to do with the possibility of reconstructing surfaces without having any other information but sampled points. The paper introduces the ϵ-sample (a sample that depends in the local feature size), a very important concept in the triangulation of surfaces that gives some properties to allow the research of good topology and geometry. In [15] the intrinsic Delaunay triangulation of a Riemannian manifold is shown to be well defined in terms of geodesics. A smooth surface embedded in $\mathbb{R}^3$ can define a Riemannian manifold, and these have the property that if all the calculations and definitions are done in a small subset of the manifold (as they can be done with a good sampling condition) the Delaunay triangulation and the Voronoi diagram are defined exactly as with the euclidean metric and are dual. In [2] the Gabriel complex is defined for $\mathbb{R}^n$. For a set of points in $\mathbb{R}^3$ the Gabriel complex is composed of triangles whose smallest defined circumsphere is free of points in the set. The advantage with [10] is that if it uses it as a 2D-Delaunay like triangulation, it does not need information about the surface. The Umbrella filter algorithm described produces topologically correct triangulations.

In [5] a study of the complexity of the Delaunay tri-angulations in surfaces is made, giving lower bounds for well distributed points in surfaces. In [9] An algorithm to sample and triangulate a surface that has correct topology and geometry is presented, but it uses computer expensive and not common operations. In [6] the concept of loose ϵ-sample is developed, it can be achieved using operations that are accessible but computer expensive. In [7] analogous for ϵ-samples and loose ϵ-samples are presented for Lipschitz surfaces. Lipschitz surfaces are more general than smooth surfaces.

In [18] an algorithm to triangulate b-reps is presented. In the algorithm all the triangulation occurs in parametric space and is mapped to $\mathbb{R}^3$. In [17] an algorithm to triangulate surfaces according to curvature and with boundary isosampled is presented. From unorganized points the problem remains unsolved. [1] is focused in the notion of envelope that is the covering of a 3-manifold created with spheres of λ size and centered in the points of the surface. From the envelope a surface with boundaries can be reconstructed, but this approach does not conserve the original points sampled in the boundary, and parameters are needed. In practice the envelope approach does not seem to produce topologically correct results. We dispose of information about the surface and boundaries and use another approach to the problem.
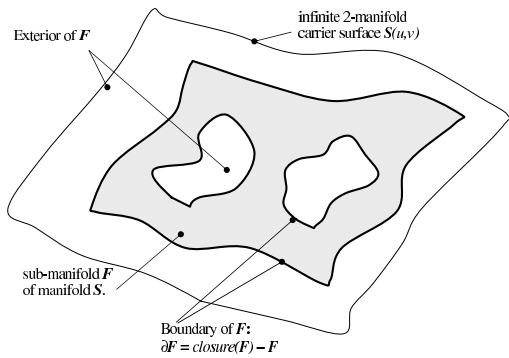
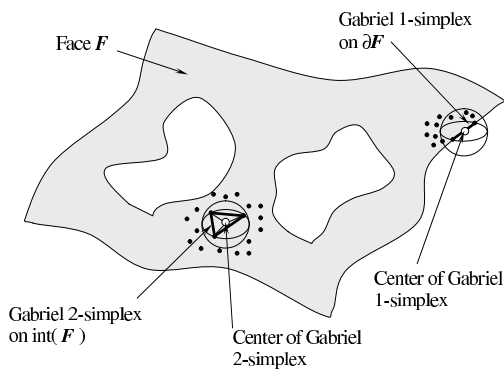Fig. 4. Interior, boundary and exterior of a submanifold F with respect to a manifold S.

Fig. 5. Gabriel 1- and 2-simplices on face F

III. METHODOLOGY

The implemented algorithm to triangulate a face F mounted onto a parametric surface S (Fig. 4) has the following layout, whose details will be discussed later: (1) Calculate the pre-image F^{-1} of the face F through the function S (Fig. 2). (2) Initialize the vertex set V_T with a curvature-sensitive sample of the loops $L_0, ..., L_n$ of the face boundary ∂F. (3) Sprinkle the face F with vertices v_i achieving a vertex density proportional to the local curvature of F, K_{max}, inserting those vertices in set V_T. (4) Calculate a Gabriel connectivity T for the vertex set V_T.

A. Edge Sampling

Algorithm 1 is used to produce a curvature - sensitive sample of an Edge E. Unlike previous approaches ([18]) such a sample is not an iso-distance one. Instead, the sampling interval at point p on the underlying curve C is sensitive to the largest of the maximal curvatures of S_1 and S_2 in such a point p (line 6). Notice that the curvature *of the curve C* at p needs not to be considered in addition to the surface curvatures because it will be always less than or equal to the surface maximal curvatures ($K_{max}(S_1, p), K_{max}(S_2, p)$).

Fig. 6 displays the geometrical idea behind lines 7 and 8 of the algorithm: the radius of curvature r is the inverse of the curvature k. A circle tangent to a curve with such a curvature may be approximated by a regular polygon of N_{sides} sides.

Algorithm 1 Sample of the Edge E between Faces F_1 and F_2

$S_1(u,v), S_2(u,v)$: Underlying surfaces for Faces F_1 and F_2.
$C(\lambda)$: Underlying Curve for E.
Λ_0, Λ_f: Parameters of the extremes of E in curve C.
V_E: Output. Sequence of point sample of E.
$K_{max}(S, p))$: Maximal curvature of Surface S at point p.
N_{sides}: Number of sides of a regular polygon.

1: $V_E = \{\}$
2: $\lambda = \Lambda_0$
3: **while** $\lambda \leq \Lambda_f$ **do**
4: $\quad p = C(\lambda)$
5: $\quad V_E = V_E \cup \{p\}$
6: $\quad k = max(K_{max}(S_1, p), K_{max}(S_2, p))$
7: $\quad r = 1/k$
8: $\quad \delta = polygon\_determined\_arc(r, N_{sides})$
9: $\quad \Delta\lambda = dist\_to\_param(\delta)$
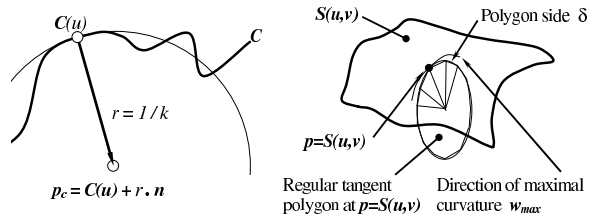10: $\quad \lambda = \lambda + \Delta\lambda$
11: **end while**

Fig. 6. Locally planar curve and local curvature. Approximation by regular polygon of N sides.

The arc δ determined by such a polygon is considered as a good euclidean sampling distance for the curve C at p (line 8). Such an euclidean distance must be transformed to a local parameter distance $\delta\lambda$ at $C(\lambda)$ (line 9).
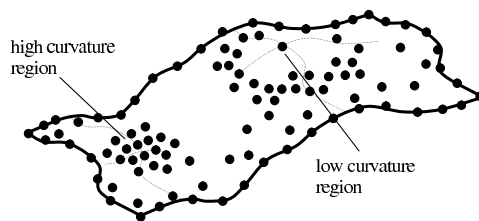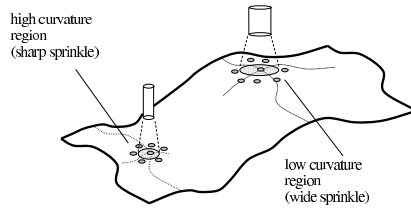

Fig. 7. Goal Point Population on face F

B. Face Sampling. Vertex Sprinkle on Face F

Algorithm 2 constructs the vertex set V_F of the triangulation sought for face F. The initialization of V_F (line 1) is done with the vertices sampled on the boundary loops of F, $\partial F = \{L_0, ..., L_n\}$, as per algorithm 1. Such vertices correctly sample ∂F. However, the interior $int(F)$ still must

Fig. 8.   Curvature-sensitive Sprinkle Airbrush F

Algorithm 2 Sprinkle triangulation vertices on Face F

F: Input. Face to triangulate.
F^{-1}: pre-image of Face F in space $U \times V$
$S(u, v)$: Underlying surface for Face F.
$\partial F = \{L_0, ..., L_n\}$: Loops Bounding the Face F.
N_f: Number of tolerated failures.
V_F: Output. Vertex set sampled on Face F.

1: V_F = sampling of boundary ∂F
2: $fails = 0$
3: **while** $fails \leq N_f$ **do**
4:    generate parameter pair $(u, v) \in F^{-1}$
5:    $k = K_{max}(S(u, v))$
6:    $r = 1/k$
7:    $p = S(u, v)$
8:    $R = polygon\_side(r, N_{sides})$
9:    **if** $\nexists q \in V_F$ such that $q \in B(p, R)$ **then**
10:       **if** $\exists v_i v_j$, a segment of the boundary, such that $p \in B_G(v_i, v_j)$ **then**
11:          $fail = fail + 1$
12:       **else**
13:          $V_F = V_F \cup \{p\}$
14:          $fail = 0$
15:       **end if**
16:    **else**
17:       $fail = fail + 1$
18:    **end if**
19: **end while**

---

be sampled. To do so, trial vertices are generated inside the pre-image F^{-1} in $U \times V$ space (line 4) and their image via S is calculated (line 7). Such a trial vertex p may be rejected if (a) it is too close to other vertices already accepted in V_F (line 11) or (b) if it is contained in the smallest ball defined by a pair of vertices consecutive on a loop L_j. The closeness criteria is dictated by the maximal curvature $K_{max}(S(u, v))$ at $p = S(u, v)$ (line 5). In the case (a) each already accepted vertex in V_f is tested for inclusion inside a ball $B(p, R)$ centered at p with radius $R = polygon\_side(r, N_{sides})$ (line 9). In the case (b) each segment $v_i v_j$ in the sample of the border is tested as a Gabriel segment (1-simplex) with respect to the candidate p. If every segment of the border is Gabriel with respect to p, we assume that p is not too close to the border (line 10). A segment is said to be sampled in the boundary, if its two end vertices are consecutive in a loop $L_j \in \partial F$. If tests (a) and (b) are passed, p is accepted in V_F

(line 13). Fig. 6 depicts that the value for R is computed as the cord of the N_{sides}-regular polygon inscribed in the circle with radius $1/k$. Function $polygon\_side(r, N_sides)$ equals to $2r \sin(\pi/N_sides)$. Fig. 5 displays the two tests mentioned in items (a) and (b) above.

C. Face Triangulation. Gabriel Connectivity on Vertex Set V_T.

Algorithm 3 Triangle Connectivity in the set V_F

V_F: Input. Vertex set sampled on Face F.
$Queue$: List of triangle edges to expand.
$\partial F = \{L_0, ..., L_n\}$: Loops Bounding the Face F.
T: Output. Triangulation.

1: $seed = triangle\_in\_interior(F)$
2: $\{(v_0, v_1), (v_1, v_2), (v_2, v_0)\} = edges\_of\_triang(seed)$
3: $Queue = \{(v_0, v_1), (v_1, v_2), (v_2, v_0)\}$
4: $T = \{ seed\}$
5: **while** $(Queue \neq \Phi)$ **do**
6:    $edge\_to\_expand = extract(Queue)$
7:    **if** $edge\_to\_expand$ is not part of the sample of the boundary **then**
8:       $(v_0, v_1) = vertices(edge\_to\_expand)$
9:       $v_{new} = vert\_for\_Gabriel\_2\_Simplex(V_F, v_0, v_1)$
10:      $T = T \cup \{(v_0, v_1, v_{new})\}$
11:      **if** $((v_0, v_{new}) \in Queue) \wedge ((v_{new}, v_1) \in Queue)$ **then**
12:         $Queue = Queue - \{(v_0, v_{new}), (v_{new}, v_1)\}$
13:      **else if** $((v_0, v_{new}) \in Queue)$ **then**
14:         $Queue = Queue - \{(v_0, v_{new})\}$
15:         $Queue = Queue \cup \{(v_1, v_{new})\}$
16:      **else if** $((v_{new}, v_1) \in Queue)$ **then**
17:         $Queue = Queue - \{(v_{new}, v_1)\}$
18:         $Queue = Queue \cup \{(v_{new}, v_0)\}$
19:      **else**
20:         $Queue = Queue \cup \{(v_1, v_{new}), (v_{new}, v_0)\}$
21:      **end if**
22:    **end if**
23: **end while**

Algorithm 3 builds the connectivity inside the vertex set V_F. The algorithm seeks to complete edges (v_0, v_1) already known to belong to the triangulation T (line 6) with an additional vertex v_{new} to build a Gabriel Triangle (v_0, v_1, v_{new}) (line 9).

Any internal Gabriel triangle is the first formed triangle (lines 1,4). It is also a seed to initialize the $Queue$ of edges potentially able to span Gabriel triangles.

If the edge extracted from the $Queue$ is part of the boundary, it is not expanded any more (line 7). All the edges part of the boundary will be found because they are 1-simplex Gabriel and make part of a 2-simplex Gabriel. If a Gabriel triangle (v_0, v_1, v_{new}) can be built, it is added to the triangulation T (line 10). If a Gabriel triangle can be built using only an existing edge (v_0, v_1) and a new vertex v_{new}, the general situation is that the new edges (v_0, v_{new}) and (v_{new}, v_1) should be queued to be eventually expanded (line 20). However, this is not always the case, since such a triangle

may use 1 or 2 *additional* edges already in the queue. In the first case, it is filling a corner (lines 13-18). In the second case, it is filling a triangular hole (lines 11,12). In such special cases additional edges (1 or 2 besides the expanded one) should be taken away from the queue.

IV. RESULTS

Several Boundary Representations B-Reps were used to test the implemented algorithm, proposed in this article. Such B-reps have genii 3 or superior, and present faces F whose underlying surfaces S are parametric ones of the NURBS or Spline types. An $N_f = 1000$ maximal number of failed trials was used to stop the sprinkle of vertices on F (generation of the set V_F). The number of sides for the approximating polygon was $N_{sides} = 30$. Figs. 9, 10 and 11 show complex B-Reps. Other examples of B-reps triangulated include a model of a pre-columbian fish in Fig. 13, a support of an axle in Fig. 14, and a stub axle in Fig. 15.

The attention of the reader is called to the fact that the connectivity construction is a process completely independent of the vertex generation one. Since the vertex generation algorithm (Sprinkle) is the most critical one, the execution time was recorded for such an aspect.

For the models *Pump* and *Hands*, Figs. 12(a) and 12(b) show execution times, corresponding to the vertex generation process. Fig. 12(c) shows the comparison of vertex generation times for such runs.

Fig. 9.   Pump carter [13]. Colormap according to quality of triangles.

V. CONCLUSIONS AND FUTURE WORK

The proposed algorithm for generating triangulation vertex sets and to calculate the connectivity among them proved to function correctly, even for very extreme geometries and topologies. Several aspects of the algorithm must be addressed: the continuity of triangle sizes at the Face Edges, the possibility of undertaking re-meshing of already existing triangulations and its related endeavor: the level of detail, applied to Finite Element Analysis. Additional research is needed in algorithms that (i) take advantage of the concepts presented in the heuristic algorithm proposed and (ii) can be proved correct.
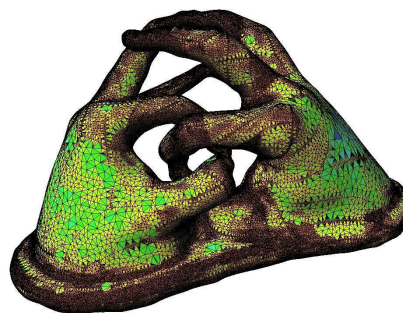

Fig. 10.   2 hands with 3 genus, scanned and reconstructed using RainDrop Geomagic. Colormap according to the size of the triangles
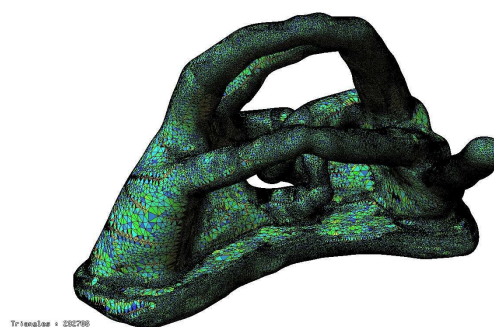

Fig. 11.   Other view of the 2 hands with 3 genus. Colormap according to the quality of the triangles.

REFERENCES

[1] K. Abe, J. Bisceglio, T. J. Peters, A. C. Russell, and T. Sakkalis. Computational topology for reconstruction of surfaces with boundary: Integrating experiments and theory. In *SMI '05: Proceedings of the International Conference on Shape Modeling and Applications 2005*, pages 290–299, Washington, DC, USA, 2005. IEEE Computer Society.

[2] Udo Adamy, Joachim Giesen, and Matthias John. New techniques for topologically correct surface reconstruction. In *VIS '00: Proceedings of the conference on Visualization '00*, pages 373–380, Los Alamitos, CA, USA, 2000. IEEE Computer Society Press.

[3] N. Amenta, M. Bern, and D. Eppstein.   The crust and the beta-skeleton: Combinatorial curve reconstruction.   *Graphical models and image processing: GMIP*, 60(2):125–, 1998.

[4] Nina Amenta and Marshall Bern.   Surface reconstruction by voronoi filtering. In *SCG '98: Proceedings of the fourteenth annual symposium on Computational geometry*, pages 39–48, New York, NY, USA, 1998. ACM.

[5] Dominique Attali, Jean-Daniel Boissonnat, and André Lieutier. Complexity of the delaunay triangulation of points on surfaces the smooth case. In *SCG '03: Proceedings of the nineteenth annual symposium on Computational geometry*, pages 201–210, New York, NY, USA, 2003. ACM.

[6] J-D Boissonnat and S. Oudot.   An effective condition for sampling surfaces with guarantees. In *SM '04: Proceedings of the ninth ACM symposium on Solid modeling and applications*, pages 101–112, Aire-la-Ville, Switzerland, Switzerland, 2004. Eurographics Association.

[7] Jean-Daniel Boissonnat and Steve Oudot. Provably good sampling and meshing of lipschitz surfaces. In *SCG '06: Proceedings of the twenty-second annual symposium on Computational geometry*, pages 337–346, New York, NY, USA, 2006. ACM.

[8] Manfredo Do Carmo.   *Differential geometry of curves and surfaces*, pages 1–168. Prentice Hall, 1976. ISBN: 0-13-212589-7.

[9] Siu-Wing Cheng, Tamal K. Dey, Edgar A. Ramos, and Tathagata Ray. Sampling and meshing a surface with guaranteed topology and geometry. In *SCG '04: Proceedings of the twentieth annual symposium*

(a)
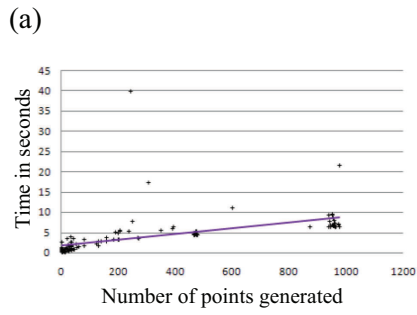
(a) Sample time per face for the pump.

(b)
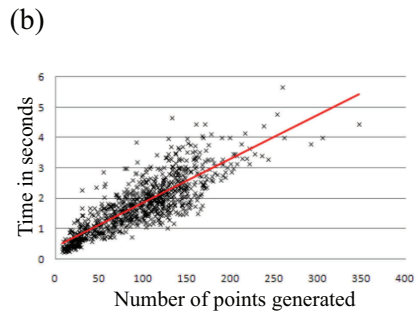
(b) Sample time per face for the two hands.

(c)
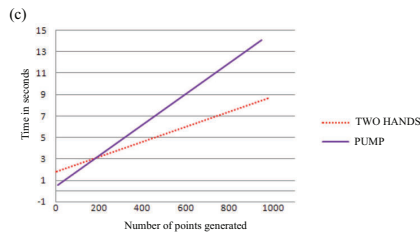
(c) Comparison between the hands (NURBS) and the Pump Carter. Hands time in solid line, Pump time in dotted line

Fig. 12.   Times spent sampling the faces and their comparison.

on Computational geometry, pages 280–289, New York, NY, USA, 2004. ACM.

[10] L. Paul Chew. Guaranteed-quality mesh generation for curved surfaces. In *SCG '93: Proceedings of the ninth annual symposium on Computational geometry*, pages 274–280, New York, NY, USA, 1993. ACM.

[11] Museo del Oro Bogotá DC. Pre-columbian fish. http://www.banrep.org/museo/eng/home4.htm.

[12] Herbert Edelsbrunner and Nimish R. Shah. Triangulating topological spaces. In *SCG '94: Proceedings of the tenth annual symposium on Computational geometry*, pages 285–292, New York, NY, USA, 1994. ACM.

[13] Rosalinda Ferrandes. Pump carter. http://shapes.aimatshape.net/viewgroup.php?id=919.

[14] Rosalinda Ferrandes. Stub axle. http://shapes.aimatshape.net/viewgroup.php?id=917.

[15] Greg Leibon and David Letscher. Delaunay triangulations and voronoi diagrams for riemannian manifolds. In *SCG '00: Proceedings of the sixteenth annual symposium on Computational geometry*, pages 341–349, New York, NY, USA, 2000. ACM.

[16] Ángel Montesdeoca. Apuntes de geometría diferencial de curvas y superficies. Santa Cruz de Tenerife, 1996. ISBN: 84-8309-026-0.

[17] Oscar E. Ruiz, John Congote, Carlos Cadavid, Juan G. Lalinde, and Guillermo Peris. Parameter-independent, curvature-sensitive sprinkle and star algorithms for surface triangulation. Submitted to the Computer-Aided Design Journal at Elsevier editorial.
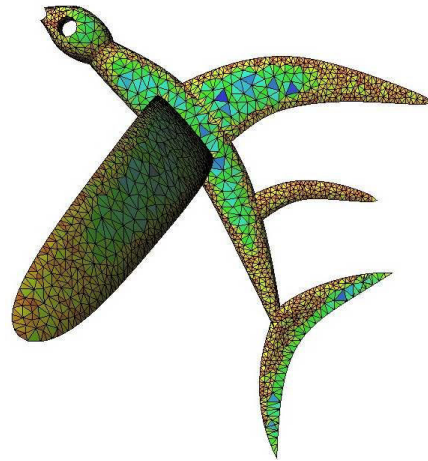
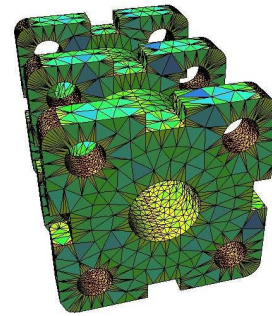Fig. 13.   Artificial replica of a pre-columbian gold fish [11]. Colormap according to size of the triangles

Fig. 14.   Support of an axle. Colormap according to size of the triangles

[18] Oscar E. Ruiz and Sebastian Peña. Aspect ratio- and size-controlled patterned triangulations of parametric surfaces. In *Ninth IASTED Intl. Conf. Computer Graphics and Imaging*, February 13-15 2007.

Fig. 15.   Stub axle [14]. Colormap according to the quality of the triangles

Prof. Dr. Eng. Oscar E. Ruiz Associate Professor Oscar Ruiz was born in 1961 in Tunja, Colombia. He obtained B.Sc. degrees in Mechanical Eng. (1983) and Computer Science (1987) at Los Andes University, Bogota, Colombia, a M.Sc. degree with emphasis in CAM (1991) and a Ph.D. with emphasis in CAD (1995) from the Mechanical & Industrial Eng. Dept. of University of Illinois at Urbana- Champaign, USA. Dr. Ruiz has held Visiting Researcher positions at Ford Motor Co. (Dearborn, USA. 1993 and 1995), Fraunhofer Inst. Graphische Datenverarbeitung (Darsmstad, Germany 1999 and 2001), University of Vigo (1999 and 2002). In 1996 Dr. Ruiz was appointed as Faculty of the Mechanical Eng. and Computer Science Depts. at EAFIT University, Medellin, Colombia, and has ever since the coordinator of the Laboratory for Interdisciplinary Research on CAD / CAM / CAE. Dr. Ruiz's interests are Computer Aided Geometric Design, Geometric Reasoning and Applied Computational Geometry. e-mail: oruiz at eafit.edu.co

Prof. Dr. Mat. Carlos Cadavid Associate Professor Carlos Cadavid was born in 1965 in Medellín, Colombia, where he obtained a bachellors degree in Mathematics at the Universidad Nacional (1988). He obtained a Masters degree from the University of Cincinnati (1990), and a Ph. D. Degree in Mathematics in 1998 from the University of Texas at Austin. He is currently a full time Faculty member at the Universidad EAFIT (Medelln). His areas of research are the topology of 4-dimensional manifolds and applications of topology to graphic computation. e-mail: ccadavid at eafit.edu.co